Deposition of LiF onto Films of Fullerene Derivatives Leads to Bulk Doping

Torabi, Solmaz; Liu, Jian; Gordiichuk, Pavlo; Herrmann, Andreas; Qiu, Li; Jahani, Fatemeh; Hummelen, Jan C.; Koster, L. Jan Anton

Published in:
ACS Applied Materials & Interfaces

DOI:
10.1021/acsami.6b05638

Publication date:
2016

ACS APPLIED MATERIALS & INTERFACES

Research Article

www.acsami.org

Deposition of LiF onto Films of Fullerene Derivatives Leads to Bulk Doping

Solmaz Torabi,*[,†] Jian Liu,[†] Pavlo Gordiichuk,[†] Andreas Herrmann,[†] Li Qiu,[†,‡] Fatemeh Jahani,[†,‡] Jan C. Hummelen,[†,‡] and L. Jan Anton Koster[†]

[†]Zernike Institute for Advanced Materials, Nijenborgh 4, 9747 AG Groningen, The Netherlands

[‡]Stratingh Institute for Chemistry, Nijenborgh 4, 9747 AG Groningen, The Netherlands

Supporting Information

ABSTRACT: One of the most commonly used cathode interlayers for increasing the efficiency of electron injection/extraction in organic electronic devices is an ultrathin layer of LiF. Our capacitance measurements and electrical conductivity analysis show that thin films of fullerene derivatives and their mixtures with polymers are unintentionally doped upon deposition of LiF. The level of doping depends on the chemical structure of the fullerene derivatives. The doping effect on polymer/fullerene mixtures is significant only for blends in which the fullerene content is greater than the polymer content by weight. Our finding has profound implications for the development and characterization of organic photovoltaic devices, including a negative impact of doping on the stability of the device and erroneous estimations of properties such as charge carrier mobility and the dielectric constant.

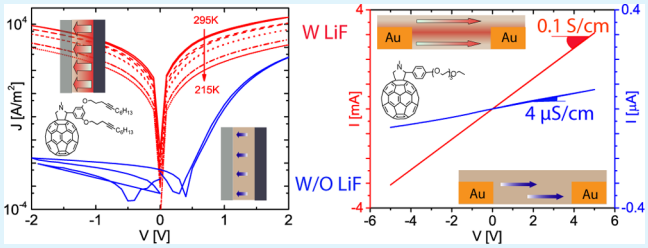

KEYWORDS: *LiF, cathode interlayers, doping, dielectric constant, charge carrier mobility, electrical conductivity, fullerene derivatives, organic solar cells*

1. INTRODUCTION

Low-work-function metals are desirable as electron-injecting/-extracting electrodes for organic electronic devices such as organic light-emitting diodes (OLEDs) and organic solar cells. However, the reactivity of these metal electrodes toward atmospheric oxygen or adjacent organic materials limits their application as stable contacts. Al, a relatively corrosion-resistant metal, is a widely used electrode material in many electronic devices. Nevertheless, the high work function of Al and its high reactivity to organic materials[1−3] make it unfavorable as a cathode material for most organic electronic devices.[4−10] For this reason, Al is normally used as a capping metal for lower-work-function metals such as Ba, Ca, or Mg.[5,6,9−11] Alkali halide interlayers are used to compensate for the high work function of Al through different electronic mechanisms.[12,13] Among these interlayer materials, LiF has attracted great interest because the incorporation of an ultrathin film (<1 nm) of LiF drastically improves the performance of photovoltaic cells and OLEDs.[4,5,7,8,14−16] Despite the wide band gap of LiF (∼13 eV),[17] which makes it a superior insulating material, an ultrathin LiF film inserted between Al and an organic film enhances the electron injection/extraction.

The underlying mechanism by which LiF interlayers improve the performance of Al cathodes is a subject of ongoing debate. We summarize the hypotheses proposed thus far into three major scenarios: (a) reduction of the barrier height for the injection of electrons through either a voltage drop at the interface or band bending,[5−7,15,18] (b) dissociation of LiF at the interface resulting in doping of the adjacent organic layer, thereby enhancing electron injection,[4,8,18−20] and (c) formation of interface dipoles, resulting in a vacuum-level downshift between the organic layer and Al.[2−4,12,20] Depending on the active layer material(s) and the techniques used to investigate their interface with LiF/Al, different scenarios have been proposed. For instance, tris(8-hydroxyquinolinato)aluminum (Alq_3) is the most extensively investigated compound for which tunneling injection,[5,6] band bending at the interface,[5,21] and doping[8,18] have been suggested as the major reasons for the enhancement of the electron injection through LiF/Al contact. For poly(9,9-dioctyl-fluorene) (PFO), the formation of a surface dipole at the PFO/LiF/Al interface has been suggested.[2] By contrast, in the case of another polyfluorene copolymer mixed with [6,6]-phenyl C_{61} butyric acid methyl ester ([60]PCBM), either Li doping of the active layer or the formation of a dipole layer at the interface has been reported.[20] In the case of solar cells with poly[2-methoxy-5-(3,7-dimethyloctyloxy)-1,4-phenylenevinylene] (MDMO-PPV):PCBM, doping of the active layer has been explicitly rejected on the basis of the observation that doping results in a substantial decrease in the photoluminescence of the fluorescent polymers.[3,12,14] Because no such degradation was observed in previous studies on poly[2-methoxy-5-(2-ethyl-

Received: May 12, 2016
Accepted: August 15, 2016
Published: August 15, 2016

DOI: 10.1021/acsami.6b05638
ACS Appl. Mater. Interfaces 2016, 8, 22623−22628

hexyloxy)-1,4-phenylenevinylene] (MEH-PPV) diodes with a LiF/Al contact,[22] LiF was concluded to similarly remain intact when in contact with MDMO-PPV:PCBM. Under this argument, however, the MDMO-PPV:PCBM blend is not directly inspected for the doping effect. Further support for the rejection of the doping scenario is based on the speculations of Heil et al.,[8] who proposed that reactions between LiF and Al can lead to the dissociation of LiF and to subsequent doping of the underlying film, independent of the composition of the film. Because secondary-ion mass spectra of both PCBM/LiF/Al and MDMO-PPV/LiF/Al interfaces showed no such reaction products,[3] LiF was concluded to remain intact at the interface. However, this argument assumes that LiF can dope the underlying film only through a reaction with Al involving dissociation of LiF.

In summary, no convincing argument disproving the doping scenario regardless of the active layer composition has been put forward. Therefore, the possibility of doping should be considered in the characterization of organic materials used in devices that require a LiF interlayer. Disentangling the extrinsic effects of LiF deposition that potentially influence the properties of the active organic compound is important. For instance, if the deposition of LiF involves the doping of the active layer, then the LiF interlayer will do more than just facilitate the injection of electrons.

In this work, we study the doping effect of LiF on different fullerene derivatives as important components of organic and perovskite solar cells. Unlike most previous studies based on interfacial spectroscopy carried out in an environment that differs from the operational conditions of a device, our work is focused on device measurements that reflect both bulk and interface properties. We study fullerene derivatives and their mixtures with polymers through capacitance and current−voltage (J−V) measurements. By investigating various fullerene derivatives, we observe that the doping effect occurs and is not specific to the chemical structure or the molecular packing of the fullerene derivatives. All of our macroscopic observations from the capacitance and current density measurements, as well as the local and bulk conductivity measurements, show that films of fullerene derivatives are doped after the deposition of a LiF layer. The extent of doping varies for different fullerene derivatives.

2. EXPERIMENTAL SECTION

Commercially available indium−tin oxide (ITO)-patterned glass substrates with different dimensions (9, 16, 36, and 100 mm^2) were used as the bottom electrode for capacitors/diodes. For in-plane capacitors/diodes, n-doped silicon substrates (doping at wafer surface: $n \approx 3 \times 10^{17} cm^{-3}$) with a 230 nm SiO_2 insulating oxide layer were used. The in-plane electrodes were patterned with 30 nm thick Au. The channel lengths were 10, 5, and 2.5 μm. The channel widths were 10 mm. The ITO substrates were cleaned by being scrubbed with a soapy water solution, flushed with deionized water, separately sonicated in acetone and isopropyl alcohol, and then oven-dried and subjected to a UV−ozone treatment. Poly(3,4-ethylenedioxythiophene) polystyrenesulfonate (PEDOT:PSS) was spin-cast under ambient conditions and dried at 140 °C for 10 min. Metallic top contacts including interlayers of LiF(1 nm), Ba (5 nm), and Ca (10 nm) were deposited at a pressure less than 10^6 mbar. To determine the capacitance, we conducted impedance spectroscopy in the frequency range from 10 Hz to 1 MHz using a Solartron 1260 impedance gain-phase analyzer with an ac drive voltage of 10 mV and an applied dc bias of −2 V or −1 V to keep the capacitors free of charge-carrier injection. The capacitance−voltage (C−V) measurements were conducted at drive frequencies of 1 and 10 kHz for Mott−Schottky analysis. Current−voltage characterizations were performed with a Keithley 2400 source meter for diodes and a Keithley 4200 for in-plane current measurements. We carried out conductive AFM (C-AFM) measurements by applying a TUNA module to a MultiMode 8 atomic force microscope (Bruker) equipped with System Controller V and operated in contact mode. NPG-10 probes with a spring constant of k = 0.06 N/m and a tip radius of 30 nm were used for the electrical measurements of both samples. Each fabricated sample was characterized using a new probe and an applied contact force less than 2 nN. All of the sample processing steps and measurements were carried out under an N_2 atmosphere at a stable temperature, except for the C-AFM measurements, which were performed under ambient conditions.

3. RESULTS AND DISCUSSION

3.1. Capacitance Measurements Reveal Doping. We studied the possible doping effect of LiF deposition on fullerene derivatives through capacitance measurements and compared the electrical capacitance of the fullerene derivatives in diodes with LiF/Al contacts to the electrical capacitance of diodes with different interlayers or without any interlayer. By dividing the capacitance of the diode by the capacitance of the corresponding empty capacitor, we calculated the relative effective dielectric constant (ε_{r-eff}) of the studied fullerene derivative. This parameter therefore reduces to the relative dielectric constant of the pristine fullerene derivative (ε_r) in the case of no doping and/or mixing. We performed Mott−Schottky analysis of the (C−V) measurements to determine the doping densities (N_D) of the affected fullerene derivatives.[23]

We started with [60]PCBM and [70]PCBM, which are the most commonly used fullerene derivatives in organic electronics, to determine the possible doping associated with LiF deposition. Figure 1a shows the variation of ε_{r-eff} of PCBM sandwiched between ITO/PEDOT:PSS and LiF/Al contacts versus the film thickness. As evident in this figure, the deposition of only 1 nm of LiF on top of the PCBM films increased their relative dielectric constants compared to those of pristine films. The values for the pristine films, as determined

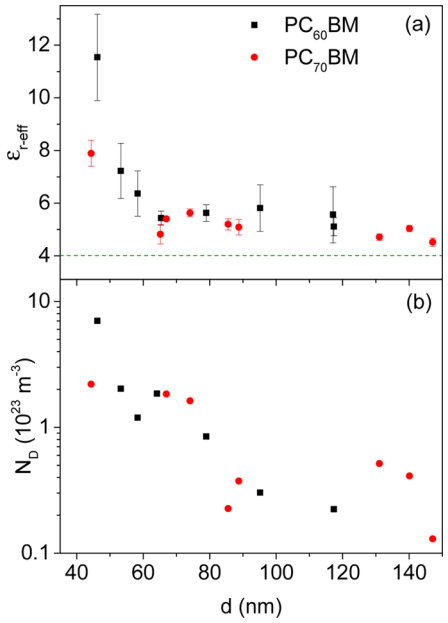

Figure 1. (a) Effective dielectric constants and (b) apparent doping densities of [60]PCBM and [70]PCBM versus the film thickness in the diode structure of ITO/PEDOT:PSS/PCBM/LiF/Al.

DOI: 10.1021/acsami.6b05638
ACS Appl. Mater. Interfaces 2016, 8, 22623−22628

from standard capacitors (without a LiF interlayer) were 4 ± 0.3 and 4.5 ± 0.3 for [60]PCBM and [70]PCBM, respectively. To quantify the doping level, we analyzed the $C-V$ results using Mott−Schottky analysis, through which we calculated the dopant density in the space charge region.[23] At thermal equilibrium, the space charge region is formed by the ionization of the dopants to provide Fermi-level alignment between the metal and the semiconductor via band bending. As shown in Figure 1b, the dopant density in the space charge region increases with decreasing film thickness. Therefore, in the case of the PCBM films, the deposition of LiF appears to provide similar amounts of dopants that can diffuse inside the film instead of remaining at the interface. Notably, the dopant density in the space charge region will be equal to the dopant density in the bulk if the doping is uniform. Therefore, the N_D values shown in Figure 1b represent the upper limits of the dopant density for all thicknesses of the bulk. Furthermore, an upper limit for the dopant density can be determined from the Mott−Schottky analysis in the case of films thinner than 100 nm.[23,24]

Table 1 lists the effective dielectric constants of [60]PCBM and [70]PCBM as extracted from the as-cast and postannealed

Table 1. Effective Dielectric Constants of PCBM Extracted from the As-Cast Diodes and from the Diodes Postannealed at 115 °C for 10 min[a]

	cathode	$\varepsilon_{r-eff} \pm 0.3$	$\varepsilon_{r-eff} \pm 0.3$ annealed
[60]PCBM (92 nm)	LiF/Al	6	12.5
	Ba/Al	4.1	4
	Al	3.9	4
[70]PCBM (70 nm)	LiF/Al	9	25.1
	Ba/Al	4.8	4.7
	Al	4.5	4.4

[a]ITO/PEDOT:PSS was used as the bottom contact for all of the diodes.

diodes fabricated with different cathodes. Postannealing clearly only influences the diodes with LiF/Al contacts, whereas diodes with Al and Ba/Al remain unaffected. Thus, annealing appears to facilitate doping.

To study the doping influence of the LiF insertion into a fullerene derivative with a different chemical structure, we used F2M (Figure 2). Unlike PCBM, F2M can be processed into

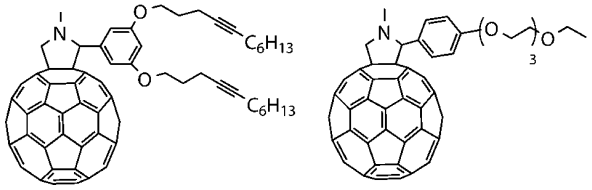

Figure 2. Chemical structures of F2M (left) and PTEG-1 (right).

uniform films with thicknesses as high as 300 nm, thus enabling us to observe whether the doping effect also occurred in thicker films. A comparison of the values of ε_{r-eff} determined from the capacitance measurements of diodes with various cathodes reveals that doping was evident only in the diodes with LiF/Al contacts (Table 2). The formation of an ohmic contact, which implies an accumulation of charges at the interface of Ca/Al and Ba/Al cathodes, also does not give rise to a substantial difference in the value of ε_{r-eff} compared with the ε_r extracted

Table 2. Apparent Doping Density and the Effective Dielectric Constants of F2M

cathode	d (nm)	$\varepsilon_{r-eff} \pm 0.3$	N_D (10^{21} m^{-3})
Ba/Al	345	3.9	0.4
Ba/Al	276	4.1	7
Ca/Al	345	4.6	
LiF/Al	280	6.8	60
LiF/Al	228	8.4	160
Al	95	3.3	
Al	231	3.7	

from standard capacitors with an Al contact. Our measurements of F2M (film thickness ∼230 nm) resulted in ε_{r-eff} values as high as 8 and doping densities similar to those of PCBM films as thin as 60 nm from capacitors with a LiF/Al contact (Table 2). Thus, F2M is apparently more strongly affected by doping than is PCBM.

To cover an even broader range of chemical structures, we chose PTEG-1 (Figure 2)[25,26] for studying the doping influence of the LiF deposition. Similarly, we aimed to find ε_{r-eff} through the capacitance measurements of PTEG-1 in the diodes with a LiF/Al contact. However, the diodes exhibited very low electrical resistances; we therefore could not determine their electrical capacitance. We instead measured the in-plane conductivity to quantify the extent of doping; the results are reported in section 3.2.3.

3.2. Current−Voltage Characterizations Reveal Doping. *3.2.1. Diodes with Different Cathodes.* $J-V$ characterization is an established method for qualifying the efficiency of electrodes. To discriminate between the electron injection enhancement effect of LiF and its doping effect, we compared the $J-V$ curves of diodes with a LiF cathode interface to those of diodes with other cathode interfaces with ohmic character. As illustrated in Figure 3a, F2M with a LiF/Al top contact

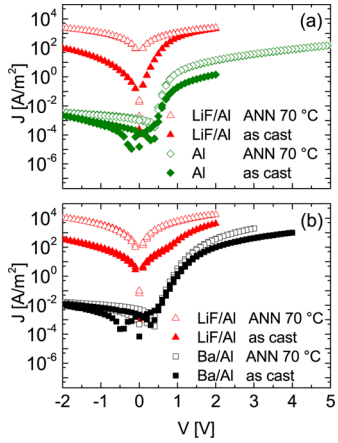

Figure 3. Current−voltage characteristics of F2M in diode structures of (a) ITO/PEDOT:PSS/F2M (230 nm)/cathode and (b) Au/PEDOT:PSS/F2M (280 nm)/cathode.

exhibits a higher current density in forward bias compared to that of F2M with an Al top contact, which can be explained by the removal of the injection barrier. However, the nearly symmetrical current density of F2M/LiF/Al cannot be explained by the asymmetry of the work function of the contacts unless doping of the active layer is involved. We observed a temperature dependence of the current in the case of the postannealed F2M/LiF/Al diodes (Figure S1); therefore,

DOI: 10.1021/acsami.6b05638
ACS Appl. Mater. Interfaces 2016, 8, 22623−22628

we expect that the symmetrical current is not due to shorts occurring in the device after annealing. We assumed that annealing facilitates ordering of the molecules, thereby enhances the transport, which increases the current density as a consequence. However, in the case of diodes with LiF/Al, annealing not only enhances the current density but also reduces the current rectification. Figure 3b shows that the influence of the LiF interlayer is not merely the elimination of injection barriers, as in the case of the Ba interlayer. The F2M diodes with identical anodes and identical active-layer thicknesses exhibit substantially different current densities. The enhanced current density for devices with a LiF/Al top contact is therefore not due to the high electron mobility of this fullerene derivative but rather is the result of doping; this effect intensifies upon postannealing of the device.

3.2.2. Role of Al Capping Layer in the Doping Effect of LiF. According to previous studies corroborating the doping scenario, LiF dopes the organic film when it is capped with Al; by contrast, in the case of capping with a noble metal, LiF remains inert.[8,20] The authors of these previous studies proposed that a reaction occurs between Al and LiF that releases Li to dope the underlying organic layer whereas no such reaction occurs with a noble metal; hence, no doping occurs.

To test this hypothesis, we designed four diodes with different configurations, as shown in the legend of Figure 4. In

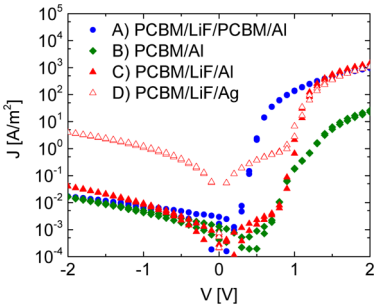

Figure 4. Current−voltage characteristics of [60]PCBM diodes with LiF at different positions compared with that of a [60]PCBM diode without LiF. The overall thicknesses of [60]PCBM in devices A−D are 140, 120, 100, and 120 nm, respectively. All four diodes have ITO/PEDOT:PSS anodes.

device A, Al and LiF layers were physically separated by a PCBM layer that prevented chemical reactions between Al and LiF. To fabricate this device, we first cast a layer of PCBM, then evaporated 0.7 nm LiF on top of it, and then cast another layer of PCBM to isolate the LiF layer from the subsequent Al film that was evaporated over all of the layers. We compared the performance of this diode with that of another diode (device C) with a configuration that enabled reactions between LiF and Al. To fabricate device C, after depositing the LiF film onto PCBM, we immediately evaporated Al to coat the whole structure. We compared the current density of these two diodes with that of another PCBM diode with an Al-only cathode (device B). As shown in Figure 4, device C, in which LiF and Al were in contact, did not exhibit a higher current density than device A, which demonstrates that a chemical reaction between Al and LiF is not necessary to initiate doping. By contrast, the current density of device A was nearly 2 orders of magnitude greater than that of B, even though both devices had an Al cathode. We attribute this greater current density of device A to the presence of LiF (0.7 nm) sandwiched between PCBM in this device, which dopes the PCBM. By contrast, in the case of device B, the PCBM remains pristine, and Al, as a Schottky contact, limits the injection of electrons, thereby leading to a lower current density. Device D, with a silver cathode, exhibited current densities similar to those of device C at voltages above the built-in voltage. This result further demonstrates that PCBM did not remain inert upon the deposition of LiF, even when capped by a noble metal.

From our local conductivity measurements via C-AFM, we derived the same conclusion as from the macroscopic $J-V$ characteristics (Figure 5). Although no Al layer was deposited

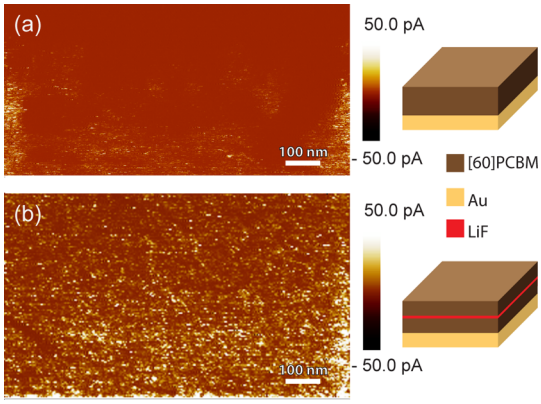

Figure 5. Local conductivity measurements of (a) pristine [60]PCBM and (b) [60]PCBM sandwiching a 0.7 nm LiF layer. The tunneling current was measured between an Au substrate and an Au tip. The scale bar at the right indicates the TUNA current according to the color code.

on top of the films, the PCBM film sandwiching a 0.7 nm LiF layer exhibited a higher tunneling current compared to that of the pristine film, indicating doping in the absence of Al.

3.2.3. Conductivity of PTEG-1 Doped with a LiF Interlayer. As discussed in section 3.1, we were unable to determine the ε_{r-eff} of PTEG-1 because of a high leakage of the capacitors with a LiF/Al contact. Therefore, we investigated the in-plane conductivity of PTEG-1 in the in-plane capacitor/diode structures shown in Figure 6a,b. We extracted a similar conductivity for the as-cast PTEG-1 film with a LiF sandwich layer and the as-cast pristine PTEG-1 (Figure S2). Through postannealing, the conductivity of the former increased by 4 orders of magnitude, whereas the latter exhibited almost no change in conductivity (Figure 6c). We cannot explain the difference in the conductivity values of PTEG-1 extracted from the in-plane diodes (Figure 6a,b) unless we consider doping originating from the LiF layers deposited onto the PTEG-1 film. Because we do not know the dopants, explaining why PTEG-1 with a LiF interlayer exhibits such a strong doping effect is difficult.

4. DEPOSITION OF LIF ONTO FILMS OF FULLERENE/POLYMER BLEND CAN LEAD TO DOPING

Because fullerene derivatives are widely used in blends with donor polymers for photovoltaics, we studied the doping effect of the insertion of a LiF layer for two types of polymer:PCBM blends. Our tests on pristine MEH:PPV and poly[(4,8-bis(2-ethylhexyloxy)-benzo(1,2-*b*:4,5-b)dithiophene)-2,6-diyl-*alt*-(4-(2-ethylhexyl)-3-fluorothieno[3,4-*b*]thiophene-)-2-carboxylate-

DOI: 10.1021/acsami.6b05638
ACS Appl. Mater. Interfaces 2016, 8, 22623−22628

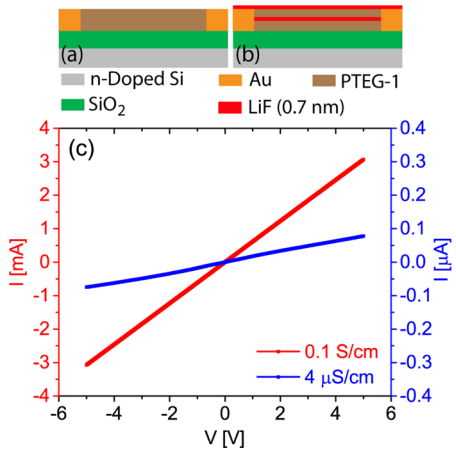

Figure 6. Cross sections of in-plane capacitors/diodes of (a) pristine PTEG-1 and (b) doped PTEG-1. (c) *I*–*V* curves of pristine (blue) and doped PTEG-1 (red) after annealing at 115 °C for 10 min. The legend shows the corresponding conductivity values.

2-6-diyl)] (PTB7) showed no evidence of doping in the device structures with a LiF/Al top contact. However, the ε_{r-eff} values that we extracted for MEH-PPV:[60]PCBM (1:4) blends from the devices with LiF/Al, Ba/Al, and Al cathodes were 4.7, 3.9, and 3.6, respectively. A comparison of these values reveals that the MEH-PPV:[60]PCBM (1:4) blend was doped in the device with a LiF/Al contact. In the case of PTB7:[70]PCBM(1:1.5), however, we observed no difference in the values of ε_{r-eff} extracted from devices with a LiF/Al contact compared with those extracted from standard devices with an Al contact. Because PCBM is the only component of the blends that is affected by the doping effect of LiF insertion, we concluded that its content in the blend may determine the level of doping. The content of PCBM was less in the PTB7:PCBM (1:1.5) blend than in the MEH-PPV:PCBM (1:4) blend; therefore, the doping appears to be insignificant in the former case. Nevertheless, regarding the complex phase composition and diffusion pathways for dopants for the polymer:PCBM blends, attributing the doping level merely to the PCBM-to-polymer weight ratio is not straightforward. We have demonstrated that doping upon deposition of LiF is likely for some polymer:PCBM films. To obtain further insights into the dependence of the doping on the phase composition of the polymer:PCBM films, a C-AFM study on the films before and after the deposition of LiF would be useful.[27]

5. POSSIBLE DOPING MECHANISMS

Our macroscopic observations reveal substantial doping associated with LiF deposition onto fullerene derivative films but cannot resolve the underlying molecular mechanism. Future spectroscopic analyses of the doped versus undoped films would provide insights into the nature of the doped species. In the following section, we speculate on the possible mechanisms underlying our observations. To this end, we note two key findings of our study: (1) The enhancement of current density and the loss of current rectification are more pronounced for the diodes with doped F2M films than they are with PCBM. Moreover, the ε_{r-eff} of doped F2M is similar to PCBM in thicker films. Therefore, F2M undergoes stronger doping than PCBM upon the deposition of LiF. (2) The conductivity of the doped PTEG-1 is sufficiently high for the measurements of in-plane current, whereas we could not measure the in-plane current of the doped PCBM beyond the noise level of our measurement equipment. Thus, the doping effect on PTEG-1 is stronger than that on PCBM. On the basis of these findings, we propose the following speculative mechanisms: (a) The stronger doping effect observed for F2M and PTEG-1 is attributable to their lower packing density caused by longer side chains. Dopants expectedly exhibit greater diffusivity in loosely packed films (F2M and PTEG-1) compared to closely packed films (PCBM). (b) The strongest doping effect that we observe for PTEG-1, compared with those of PCBM and F2M, suggests that a form of Li (i.e., Li atoms, as in the metal) could be active as n-doping agent(s) in the described experiments. When the fullerene cage is reduced by Li, the resulting Li^+ ions can then be solvated by the ethyleneoxy groups. However, formation of Li from LiF seems quite unlikely. (c) Because postannealing facilitates further doping in all cases, we conclude that the doping does not merely occur throughout the deposition of LiF but that the dopants remain active in the film after the deposition. Apparently, annealing activates further reactions, which lead to additional doping or facilitate diffusion of the dopants deeper inside the fullerene film.

6. CONCLUSIONS

We have shown that the evaporation of LiF onto thin films of fullerene derivatives leads to bulk doping. The level of unintentional doping varies depending on the chemical structure of the fullerene derivatives and their matrix in the film. The presence of Al is not necessary to activate the doping, as indicated by our observation of the doping effect in the films without a metallic contact. We also observed that annealing possibly facilitates the doping by enabling easier diffusion into the bulk, leading to the doping of additional fullerene molecules. Because we did not observe the doping of pristine polymers, we conclude that the mixtures of polymer:fullerene show the doping effect only because of the presence of the fullerene molecules.

Our results have important implications for organic electronic devices because we have shown that the intrinsic properties of fullerene derivatives can substantially deviate from their pristine values when extracted from devices incorporating LiF interlayers. Moreover, the devices containing fullerene derivatives may face stability issues because of the unintentional doping effect of LiF deposition. Alkali metals and their salt or alloy compounds can give rise to unintentional doping similar to LiF, which should be investigated in future works.

■ ASSOCIATED CONTENT

Supporting Information

The Supporting Information is available free of charge on the ACS Publications website at DOI: 10.1021/acsami.6b05638.

Temperature dependent current–voltage characteristics of doped F2M, before and after annealing. In-plane current–voltage characteristics of pristine and doped PTEG-1 before and after annealing. (PDF)

■ AUTHOR INFORMATION

Corresponding Author

*E-mail: s.torabi@rug.nl. Phone: +31 (0)50 3635211.

Notes

The authors declare no competing financial interest.

DOI: 10.1021/acsami.6b05638
ACS Appl. Mater. Interfaces 2016, 8, 22623–22628

■ ACKNOWLEDGMENTS

This work was supported through Foundation for Fundamental Research on Matter (FOM), by grant FOM-G-23. This is a publication by the FOM Focus Group "Next Generation Organic Photovoltaics", participating in the Dutch Institute for Fundamental Energy Research (DIFFER). We acknowledge Dr. A. Mashaghi for comments that greatly improved the manuscript.

■ REFERENCES

(1) Kahn, A.; Koch, N.; Gao, W. Electronic Structure and Electrical Properties of Interfaces Between Metals and π-conjugated Molecular Films. *J. Polym. Sci., Part B: Polym. Phys.* **2003**, *41*, 2529−2548.
(2) Greczynski, G.; Fahlman, M.; Salaneck, W. R. An Experimental Study of (9, 9-dioctyl-fluorene) and Its Interfaces with Li, Al, and LiF. *J. Chem. Phys.* **2000**, *113*, 2407−2412.
(3) Van Gennip, W.; Van Duren, J.; Thüne, P.; Janssen, R.; Niemantsverdriet, J. he Interfaces of Poly (p-phenylene Vinylene) and Fullerene Derivatives with Al, LiF, and Al/LiF Studied by Secondary Ion Mass Spectroscopy and X-ray Photoelectron Spectroscopy: Formation of AlF3 Disproved. *J. Chem. Phys.* **2002**, *117*, 5031−5035.
(4) Shaheen, S.; Jabbour, G.; Morrell, M.; Kawabe, Y.; Kippelen, B.; Peyghambarian, N.; Nabor, M.-F.; Schlaf, R.; Mash, E.; Armstrong, N. Bright Blue Organic Light-emitting Diode with Improved Color Purity Using a LiF/Al Cathode. *J. Appl. Phys.* **1998**, *84*, 2324−2327.
(5) Hung, L.; Tang, C.; Mason, M. Enhanced Electron Injection in Organic Electroluminescence Devices Using an Al/LiF Electrode. *Appl. Phys. Lett.* **1997**, *70*, 152−154.
(6) Jabbour, G.; Kawabe, Y.; Shaheen, S.; Wang, J.; Morrell, M.; Kippelen, B.; Peyghambarian, N. Highly Efficient and Bright Organic Electroluminescent Devices with an Aluminum Cathode. *Appl. Phys. Lett.* **1997**, *71*, 1762−1764.
(7) Matsumura, M.; Furukawa, K.; Jinde, Y. Effect of Al/LiF Cathodes on Emission Efficiency of Organic El Devices. *Thin Solid Films* **1998**, *331*, 96−100.
(8) Heil, H.; Steiger, J.; Karg, S.; Gastel, M.; Ortner, H.; Von Seggern, H.; Stößel, M. Mechanisms of Injection Enhancement in Organic Light-emitting Diodes Through an Al/LiF Electrode. *J. Appl. Phys.* **2001**, *89*, 420−424.
(9) Steim, R.; Kogler, F. R.; Brabec, C. J. Interface Materials for Organic Solar Cells. *J. Mater. Chem.* **2010**, *20*, 2499−2512.
(10) Chen, L.-M.; Xu, Z.; Hong, Z.; Yang, Y. Interface Investigation and Engineering−achieving High Performance Polymer Photovoltaic Devices. *J. Mater. Chem.* **2010**, *20*, 2575−2598.
(11) Nikiforov, M. P.; Strzalka, J.; Jiang, Z.; Darling, S. B. Lanthanides: New Metallic Cathode Materials for Organic Photovoltaic Cells. *Phys. Chem. Chem. Phys.* **2013**, *15*, 13052−13060.
(12) Shaheen, S. E.; Brabec, C. J.; Sariciftci, N. S.; Jabbour, G. E. Effects of Inserting Highly Polar Salts Between the Cathode and Active Layer of Bulk Heterojunction Photovoltaic Devices. *MRS Online Proc. Libr.* **2001**, *665*, C5−C51.
(13) Lin, F.; Liu, X.; Li, Y.; Hu, Y.; Guo, X. Ultrathin Metal Fluoride Interfacial Layers for Use in Organic Photovoltaic Cells. *Adv. Funct. Mater.* **2015**, *25*, 6906−6912.
(14) Brabec, C. J.; Shaheen, S. E.; Winder, C.; Sariciftci, N. S.; Denk, P. Effect of LiF/metal Electrodes on the Performance of Plastic Solar Cells. *Appl. Phys. Lett.* **2002**, *80*, 1288−1290.
(15) Brown, T.; Friend, R.; Millard, I.; Lacey, D.; Burroughes, J.; Cacialli, F. Efficient Electron Injection in Blue-emitting Polymer Light-emitting Diodes with LiF/Ca/Al Cathodes. *Appl. Phys. Lett.* **2001**, *79*, 174−176.
(16) Brown, T.; Friend, R.; Millard, I.; Lacey, D.; Burroughes, J.; Cacialli, F. LiF/Al Cathodes and the Effect of LiF Thickness on the Device Characteristics and Built-in Potential of Polymer Light-emitting Diodes. *Appl. Phys. Lett.* **2000**, *77*, 3096−3098.
(17) Milgram, A.; Givens, M. P. Extreme Ultraviolet Absorption by Lithium Fluoride. *Phys. Rev.* **1962**, *125*, 1506.
(18) Le, Q. T.; Yan, L.; Gao, Y.; Mason, M.; Giesen, D.; Tang, C. Photoemission Study of Aluminum/tris-(8-hydroxyquinoline) Aluminum and Aluminum/LiF/tris-(8-hydroxyquinoline) Aluminum Interfaces. *J. Appl. Phys.* **2000**, *87*, 375−379.
(19) Kido, J.; Matsumoto, T. Bright Organic Electroluminescent Devices Having a Metal-doped Electron-injecting Layer. *Appl. Phys. Lett.* **1998**, *73*, 2866−2868.
(20) Jönsson, S.; Carlegrim, E.; Zhang, F.; Salaneck, W. R.; Fahlman, M. Photoelectron Spectroscopy of the Contact Between the Cathode and the Active Layers in Plastic Solar Cells: The Role of LiF. *Jpn. J. Appl. Phys.* **2005**, *44*, 3695.
(21) Lee, J.; Park, Y.; Kim, D.; Chu, H.; Lee, H.; Do, L.-M. High Efficiency Organic Light-emitting Devices with Al/NaF Cathode. *Appl. Phys. Lett.* **2003**, *82*, 173−175.
(22) Yang, X.; Mo, Y.; Yang, W.; Yu, G.; Cao, Y. Efficient Polymer Light Emitting Diodes with Metal Fluoride/Al Cathodes. *Appl. Phys. Lett.* **2001**, *79*, 563−565.
(23) Kirchartz, T.; Gong, W.; Hawks, S. A.; Agostinelli, T.; MacKenzie, R. C.; Yang, Y.; Nelson, J. Sensitivity of the Mott−schottky Analysis in Organic Solar Cells. *J. Phys. Chem. C* **2012**, *116*, 7672−7680.
(24) Nigam, A.; Premaratne, M.; Nair, P. R. On the Validity of Unintentional Doping Densities Extracted Using Mott−schottky Analysis for Thin Film Organic Devices. *Org. Electron.* **2013**, *14*, 2902−2907.
(25) Torabi, S.; Jahani, F.; Van Severen, I.; Kanimozhi, C.; Patil, S.; Havenith, R. W. A.; Chiechi, R. C.; Lutsen, L.; Vanderzande, D. J. M.; Cleij, T. J.; Hummelen, J. C.; Koster, L. J. A. Title Case Strategy for Enhancing the Dielectric Constant of Organic Semiconductors Without Sacrificing Charge Carrier Mobility and Solubility. *Adv. Funct. Mater.* **2015**, *25*, 150−157.
(26) Jahani, F.; Torabi, S.; Chiechi, R. C.; Koster, L. J. A.; Hummelen, J. C. Fullerene Derivatives with Increased Dielectric Constants. *Chem. Commun.* **2014**, *50*, 10645−10647.
(27) Nikiforov, M. P.; Darling, S. B. Improved Conductive Atomic Force Microscopy Measurements on Organic Photovoltaic Materials via Mitigation of Contact Area Uncertainty. *Prog. Photovoltaics* **2013**, *21*, 1433−1443.

DOI: 10.1021/acsami.6b05638
ACS Appl. Mater. Interfaces 2016, 8, 22623−22628